

# Cationic Glyconanoparticles: Their Complexation with DNA, Cellular Uptake, and Transfection Efficiencies

Marya Ahmed,<sup>†,‡</sup> Zhicheng Deng,<sup>†,‡</sup> Shiyong Liu,<sup>§</sup> Robert Lafrenie,<sup>||</sup> Aseem Kumar,<sup>‡</sup> and Ravin Narain<sup>\*,†,‡</sup>

Department of Chemical and Materials Engineering, University of Alberta, Edmonton, Alberta, T6G 2G6, Canada, Department of Chemistry and Biochemistry, Biomolecular Sciences Program, Laurentian University, 935, Ramsey Lake Road, Sudbury, Ontario, P3E 2C6, Canada, Department of Polymer Science and Engineering, University of Science and Technology of China, Hefei, Anhui, China, and Regional Cancer Program of the Hospital, 41 Ramsey Lake Road, Sudbury, Ontario, Canada. Received August 6, 2009; Revised Manuscript Received September 16, 2009

There is a need to synthesize new gene delivery vehicles that can deal with the problems of endosomal escape and nuclear entry. We propose cationic glycopolymer-stabilized gold nanoparticles as an effective gene delivery system. The cationic glyconanoparticles synthesized were revealed to be biocompatible and are resistant to aggregation in physiological conditions. The complexation of DNA to the cationic glyconanoparticles is determined by agarose gel electrophoresis. The localization of the DNA-glyconanoparticles inside the Hela cell line and their mechanism of uptake is studied by confocal microscopy. Finally, the efficacy of the glyconanoparticles as gene delivery vehicles *in vitro* is studied by their complexation with cyanine fluorescence protein encoded plasmid, and the transfection efficiency is found to be comparable to the commercially available control Lipofectamine 2000.

## INTRODUCTION

Safety issues associated with viral gene delivery vehicles have led to the popularization of a variety of nonviral gene delivery vehicles, such as liposomes, cationic polymers, nanoparticles, and dendrimers (1–10). Another approach recommends the use of hybrid viral vehicles that are shown to produce high efficacy *in vitro*; however, the safety concerns associated with them cannot be ignored (11). In nonviral gene delivery vehicles, compared to those of lipoplex systems, polyplex-based ones can effectively promote vesicular escape and nuclear entry (12, 13). Polyethylenimine (PEI), despite its high toxicity, has been largely utilized as an effective gene delivery vehicle (1). Chitosan, a glucosamine-based polymer, is completely nontoxic and shows relatively low transfection efficiencies (1). The different chitosan modification approaches, including PEGylation and amination, have been reported to overcome the issues of gene delivery associated with these vectors (1). Reineke et al. has combined the high transfection abilities of PEI with low toxicity of chitosan, by synthesizing cationic glycopolymers of defined molecular weight, which show enhanced gene transfer ability with reduced toxicity (14). It has also been demonstrated that cationic polymer coated metallic nanoparticle-DNA complexes show enhanced gene transfer ability due to better DNA binding ability and increased stability in physiological conditions than their corresponding polyplexes (15–17). Although various macromolecule stabilized gold nanoparticles have been synthesized and their biological and chemical properties are reported (18–22), only a handful of papers discuss the *in vitro* uses of cationic gold nanoparticles as gene delivery systems (7, 8, 17, 23, 24). The use of gold

nanoparticles as gene delivery vehicles is either facilitated by external forces or associated with significantly low transfection efficiencies, due to the possible entrapment of PEG-modified vehicles inside the endosomes (7, 8). Carbohydrate functionalized gold nanoparticles, also known as glyconanoparticles, are not only interesting due to their PEG-like biocompatibility, but are also found to be involved in cell-mediated interactions (25–27). The aforementioned strategies when combined can produce monodisperse, biocompatible, cationic glyconanoparticles as gene delivery vehicles that can enhance the cellular uptake by cell mediated interactions and lack the drawbacks of PEG stabilized vehicles, thus promoting higher transfection efficiencies (3, 4, 28). We have previously reported the comparison between transfection efficiencies of cationic glyconanoparticles of different core sizes (29). However, a complete study on the synthesis of cationic glyconanoparticles prepared by UV radiation, their size control as a function of ligand concentrations and UV light intensity, and their mechanism of interactions with living cells has not yet been reported in detail (29).

Herein, we report a facile one-step synthesis of cationic glyconanoparticles as an effective gene delivery system. Well-defined cationic glycopolymers were first synthesized by the reversible addition–fragmentation chain transfer (RAFT) process and their cytotoxicity was determined. The cationic glyconanoparticles were then produced in one step using UV radiation (Scheme 1).

Photoirradiation process for the synthesis of unprotected gold nanoparticles, introduced by Scaiano et al., has been widely investigated (30–32). We have successfully synthesized the mixed monolayer stabilized gold nanoparticles using this technique (31, 32). The synthesis of cationic gold nanoparticles is achieved using the photoinitiator, Irgacure-2959, and the effect of concentration of glycopolymer and of the intensity of radiation on the size and polydispersity of nanoparticles is studied. The monodisperse cationic gold nanoparticles produced are further complexed with fluorescence-labeled oligonucleotides, and the confocal microscopy is performed to study the

\* Corresponding author. narain@ualberta.ca or rnarain@laurentian.ca; Tel: +1 780 492 1736 or +1 705 675 1151 (2186); Fax: +1 780 492 2881 or +1 705 675 4844.

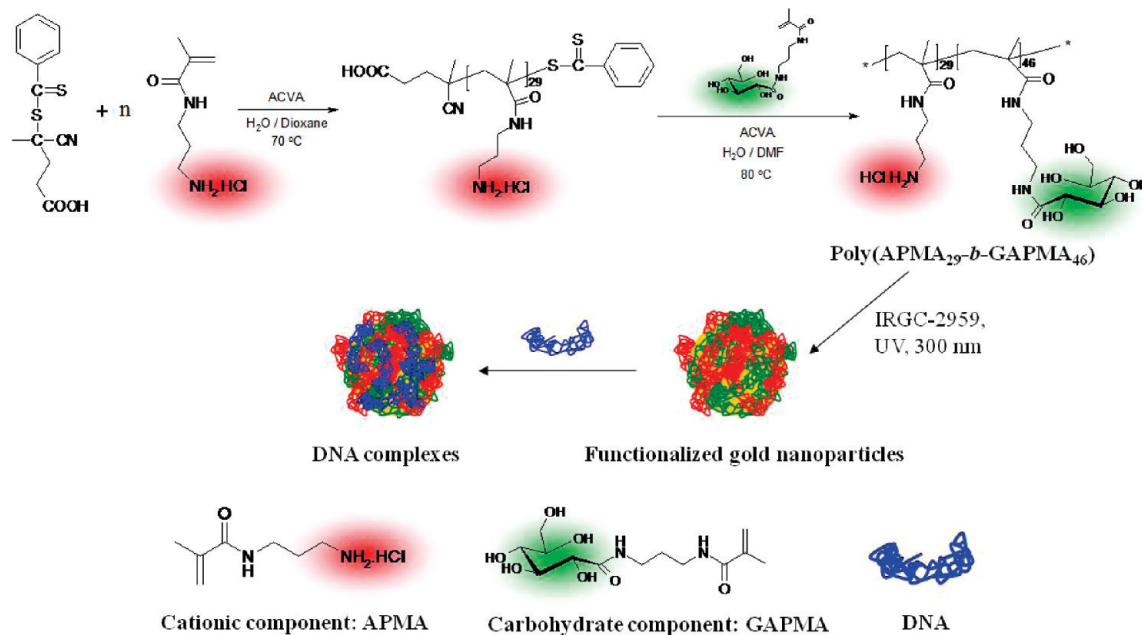
<sup>†</sup> University of Alberta.

<sup>‡</sup> Laurentian University.

<sup>§</sup> University of Science and Technology of China.

<sup>||</sup> Regional Cancer Program of the Hospital.

Scheme 1. Synthesis of the Diblock Copolymer, Formation of Cationic Glyconanoparticles, and Their Complexation with DNA



mechanism of uptake of novel gene carrier and their colocalization in human cells. The pECFP plasmid is complexed with the cationic gold nanoparticles, and agarose gel electrophoresis is performed to determine the net charge on the surface of nanoparticles–plasmid complex. Finally, the transfection efficiency of the carrier with net positive charge is demonstrated in HeLa cells, and it is found that cationic glyconanoparticles exhibit high transfection efficiencies with significantly low toxicity.

## MATERIALS AND METHODS

**Materials.** All chemicals were purchased from Sigma-Aldrich and were used without purification.

**Methods. Polymer Characterization.** <sup>1</sup>H NMR spectra of the monomers and polymers were recorded on a Varian 200 MHz instrument.

Molecular weight and molecular weight distributions were determined by a conventional Viscotek gel permeation chromatography (GPC) system using aqueous eluents, two Waters WAT011545 columns at room temperature, and a flow rate of 1.0 mL/min using a 0.5 M sodium acetate/0.5 M acetic acid buffer as eluent. p(APMA) was characterized based on six near-monodisperse PEO standards ( $M_p = 1010$ – $101\,200$  g mol<sup>−1</sup>). p(APMA-*b*-GAPMA) was characterized based on seven near-monodisperse Pullulan standards ( $M_w = 5900$ – $404\,000$  g mol<sup>−1</sup>).

**Dynamic Light Scattering (DLS).** Dynamic light scattering measurements were performed at room temperature using a Viscotek DLS instrument having a He–Ne laser at a wavelength of 632 nm and Peltier temperature controller. p(APMA-*b*-GAPMA) stabilized gold nanoparticle solutions were filtered through Millipore membranes (0.45 μm pore size). The data were recorded with Omni Size Software.

**UV–vis Spectroscopy.** UV–vis absorption spectra (400–800 nm) were recorded on a Cary UV 100 spectrophotometer from the aqueous solutions of p(APMA-*b*-GAPMA) gold nanoparticles at room temperature.

**Confocal Microscopy.** The fluorescent images were obtained using Zeiss LSM 510 Meta confocal microscope with 63× objective. The wavelengths of excitation and emission used were 552 and 575 nm, respectively.

**Plasmid Preparation and Purification.** pECFP-N1, enhanced cyan fluorescent plasmid driven by cytomegalovirus (CMV) promoter, was transformed in super competent *E. coli* cells and was amplified in 30 μg/mL Kanamycin containing LB broth media at 37 °C overnight with 225 rpm. After sufficient bacterial growth, the cells were pelleted by centrifugation at 2000g and 20 °C for 5 min followed by plasmid extraction using QIAGEN mini plasmid purification kit as per vendor's protocol. Plasmid purity was assessed by UV spectrophotometry ( $A_{260/280} > 1.75$ ) and agarose gel electrophoresis.

**Block Copolymerization of APMA with GAPMA.** *Diblock Copolymerization of 3-Aminopropyl Methacrylamide Hydrochloride (APMA) with 3-Gluconamidopropyl Methacrylamide (GAPMA) via Reversible Addition–fragmentation Chain Transfer Process (RAFT).* APMA was first polymerized using 4-cyanopentanoic acid dithiobenzoate (CTP) as chain transfer agent (CTA) and 4,4'-azobis(4-cyanovaleric acid) (ACVA) as initiator according to the previous report (37). Detail protocol was as follows: in a 10 mL Schlenk flask, APMA (2 g, 11.2 mmol) was dissolved in double distilled water (4 mL) before the addition of 2 mL CTP (52 mg, 0.186 mmol, target  $DP_n = 60$ ) and ACVA (16 mg, 0.038 mmol) 1,4-dioxane stock solution. After degassing via three freeze–thaw cycles, the flask was placed in a preheated oil bath to initiate the polymerization at 70 °C. After 3 h 45 min, the polymerization was quenched at 50% conversion. Resulting polymer was precipitated in acetone, and the residual monomer was removed by washing with 2-propanol. Subsequently, poly (APMA) ( $M_n = 5200$  g·mol<sup>−1</sup>;  $M_w/M_n = 1.23$ ) was used as macro chain transfer agent (Macro-CTA) to synthesize p(APMA-*b*-GAPMA) diblock copolymer. As the second monomer, GAPMA (0.95 g) was added to p(APMA) solution (0.5 g in 7.5 mL double distilled water) followed by the addition of 0.1 mL ACVA (7.5 mg) *N,N*-dimethylformamide (DMF) stock solution. After degassing via three freeze–thaw cycles, the flask was placed in a preheated oil bath for 20 h at 80 °C. The diblock copolymer p(APMA-*b*-GAPMA) was precipitated in acetone followed by washing with methanol.

**Synthesis of Block Copolymer Coated Au Nanoparticles in the Presence of Irgacure-2959 (IRGC).** p(APMA-*b*-GAPMA) coated gold nanoparticles were synthesized by photoirradiation using Irgacure-2959 (IRGC) as a

photoinitiator. The molar ratios of  $\text{HAuCl}_4$ , IRGC, and p(APMA-*b*-GAPMA) in deionized water were 1:3:0.01, 1:3:0.02, or 1:3:0.05. p(APMA-*b*-GAPMA) with molecular weights 19.9 kDa (2.5 mg), 25 kDa (3.3 mg), were used. In a typical synthesis, required amount of p(APMA-*b*-GAPMA) were dissolved in deionized water and solution was added to  $\text{HAuCl}_4$  (0.50 mg/mL) solution in deionized water. The mixture was stirred using a magnetic stirrer at room temperature for 20 min. Irgacure-2959 (15.3 mM, 1 mL) was dissolved in the mixture of deionized water and MeOH (4:1, v/v). The initiator solution was then added to the  $\text{HAuCl}_4$  and p(APMA-*b*-GAPMA) mixture was stirred for 20 min. The photoirradiation of the reaction mixture was carried out using sixteen, twelve, eight, and four 75 W UV lamps at wavelength a 300 nm in a Rayonet photoreactor (Southern N.E. Ultraviolet Co.) After 5 min, the reaction mixture was taken off the photoreactor and stirred at room temperature. The gold nanoparticles produced were centrifuged at 20 000 rpm for 2 h to remove the excess of polymer. The pellet was resuspended in deionized water.

**Serum Assay.** The cationic glycopolymer stabilized gold nanoparticles of size 6 nm were resuspended in deionized water, phosphate buffer saline, and 10% v/v human serum separately to achieve the final concentration of 2.5  $\mu\text{M}$  in each solution. Then, the change in size of gold nanoparticles was measured by UV-vis spectroscopy in the wavelength range 400–700 nm and by dynamic light scattering instrument.

**DNA Complexation.** DNA complexation of gold nanoparticles was studied using agarose gel electrophoresis. The varying concentrations of gold nanoparticles (45, 89, 139, 196  $\mu\text{M}$ ) were complexed with 340 ng of pECFP-N1 plasmid and the complexes were loaded into 0.7% agarose gel. The gel was run for 1 h at 70 V, and the complexes were characterized after staining the gel with 0.5  $\mu\text{g/mL}$  of ethidium bromide. The images were obtained on an ultraviolet transilluminator.

**Confocal Microscopy.** Hela cells were grown in Dulbecco's modified eagle medium, DMEM containing 10% fetal bovine serum, and 1% penicillin/streptomycin in a humidified atmosphere with 5%  $\text{CO}_2$  at 37 °C. Upon 80% confluency, cells were trypsinized and neutralized with equal amounts of medium. The cells were then reseeded in a 6 well plate, in which each well contained sterile glass coverslips. The plate was incubated in humidified atmosphere at 37 °C, and upon 80% confluency, 1.3 mM nanoparticles complexed with 1.1  $\mu\text{M}$  TAMARA dye labeled oligonucleotides containing medium were introduced in chambered cover glass. The other two wells served as controls, containing no treatment and 1.1  $\mu\text{M}$  TAMARA labeled oligonucleotides in the medium, respectively. The cells were further incubated for 3 h at 37 °C. The growth medium was then removed, and cells were washed several times with phosphate buffer saline. The cells were fixed with 4% *p*-formaldehyde solution at room temperature for 5 min, followed by washing with Dulbecco's phosphate buffer saline (DPBS). The cover glass was then mounted on a microscopic glass slide and was studied under the microscope.

**Mechanism of Uptake of Gold Nanoparticles by Human Cell Line.** *Temperature Dependent Uptake of Gold Nanoparticles.* The energy dependent uptake of TAMARA labeled gold nanoparticles was studied using the same procedure as described before (35). In summary, the cells were seeded in 6 well plates, containing glass coverslips. The plate was incubated in humidified atmosphere at 37 °C for 24 h. The medium was removed and was replaced with 9.5  $\mu\text{M}$  nanoparticles complexed with 1.1  $\mu\text{M}$  TAMARA labeled oligonucleotides containing medium. The plate was then incubated for 3 h at 4 °C. The cells were then washed several times with DPBS and fixed with 4% *p*-formaldehyde. The coverslip was then finally washed with

DPBS and was mounted on microscopic glass slide. The glass slide was studied under confocal microscope.

*Clathrin Dependent Uptake of Gold Nanoparticles.* Hela cells were seeded in 6 well plates as described above; upon 80% confluency, the cells were pretreated with 0.45 M sucrose containing medium for 30 min at 37 °C. The medium was removed and cells were washed several times with DPBS. The medium containing 9.5  $\mu\text{M}$  nanoparticles complexed with 1.1  $\mu\text{M}$  TAMARA labeled oligonucleotides was added and cell were further incubated for 3 h. The cells were washed with DPBS and fixed with *p*-formaldehyde. The coverslip was mounted on a microscopic glass slide to study under confocal microscope.

**Transfection.** Hela cells were maintained in Dulbecco's modified Eagles' medium, supplemented with 10% fetal bovine serum at 37 °C, in a humidified 5%  $\text{CO}_2$  atmosphere, as described above. Before the experiment, 2000 Hela cells were seeded on a 96 well tissue culture plate and were allowed to adhere overnight. The test samples were prepared for each well by mixing 0.35  $\mu\text{g}$  of CFP plasmid with varying amounts of cationic gold nanoparticles. The mixture was incubated for 15 min and was added to the cells; the plate was incubated for 6 h at 37 °C, in serum free medium. The cells were washed three times with DPBS and were allowed to grow for another 48 h in fresh culture medium supplemented with 10% FBS. The gene expression was evaluated using fluorescent microscopy. The presence of CFP protein was confirmed using the emission spectrum of cyanine fluorescence protein at 490 nm.

**Toxicity Assays.** *Toxicity Assay for Glycopolymer. 1. Preparation of Polymer Stock Solutions.* All polymers were dissolved into Dulbecco's phosphate buffer at the final concentration of 0.6 mM. The samples were autoclaved, and different volumes of prepared solution were added into different volumes of DMEM medium to obtain the final concentrations of 2, 4, and 6  $\mu\text{M}$  concentration of polymer in the medium.

*2. Cytotoxicity Test.* Cytotoxicity was characterized using MTT assay. Hela cells were plated in 96 well plates at density of 15 000 cells/well in 100  $\mu\text{L}$  of serum and antibiotic supplemented growth medium. Cells were incubated for 24 h at 37 °C and 5%  $\text{CO}_2$ , after which time the growth medium was replaced with DMEM medium containing different concentrations of polymers, prepared above (pAPMA) and p(APMA-*b*-GAPMA). The cells were further incubated for 24 h under the same conditions, after which 25  $\mu\text{L}$  of MTT dye was added to each well and plate was incubated for 2 h. Next, 100  $\mu\text{L}$  of MTT lysis solution was added to each well, and cells were incubated overnight. Absorbance was measured at 570 nm. Survival percentage was calculated by comparison to untreated cells (100% survival).

*Toxicity Assay on Transfected Cells.* Hela cells maintained at 80% confluency were seeded at 2000 cells/well in 96 well plate and were allowed to adhere overnight. The varying concentrations of gold nanoparticle–plasmid complex in serum free medium were added to each well, and each experiment was done in triplicate. After 6 h, the medium was changed to serum containing medium, and cells were allowed to grow for another 48 h. The cell viability was tested using MTT assay, as described above.

## RESULTS AND DISCUSSION

The carbohydrate molecules present on the surface of cells are involved in a variety of biological functions, including cellular recognition, cell adhesion, and cell growth regulation. The polyvalent interactions between carbohydrate–carbohydrate molecules and carbohydrate–protein molecules on the surface of a pathogen lead to their uptake by a living cell (25–27). These specific carbohydrate based cellular interactions can be exploited to design novel carriers for the gene and drug delivery purposes. A variety of protein and peptide stabilized nanopar-



**Table 1. Dynamic Light Scattering Data Showing the Size Control of Gold Nanoparticles as a Function of Ligand Concentration**

entry	polymer conc. [M]	molar ratio Au:I:Polymer	intensity (W)	mass dist.	size PDI
1	$2.2 \times 10^{-4}$	1:3:0.05	224	8.24	0.18
2	$1.1 \times 10^{-4}$	1:3:0.02	224	14.85	0.21
3	$5.1 \times 10^{-5}$	1:3:0.01	224	2.9	0.23
4	$5.1 \times 10^{-6}$	1:3:0.005	224	3.7	0.13

ticles have been reported and their uptake by human cells is studied (12, 17). The studies have also shown that endosomal entrapment is also a major hindrance in the success of other gene delivery vehicles (10). The synthesis of cationic glyconanoparticles of 10 nm core diameter using cationic glycopolymer p(APMA<sub>31</sub>-b-LAEMA<sub>32</sub>), has been previously reported (29); herein, we present a detailed study of the synthesis of cationic glycopolymer stabilized gold nanoparticles, using cationic glycopolymer p(APMA-b-GAPMA) of different molecular weights by photochemistry. The gold nanoparticles produced are stabilized with the diblock cationic glycopolymer p(APMA<sub>31</sub>-b-GAPMA<sub>45</sub>) that serves a variety of purposes. The glycopolymer segment imparts the biocompatibility and mediates the cellular interactions with nanoparticles, while the cationic moiety provides the complexation of anionic macromolecules on the surfaces of nanoparticles. The synthesized cationic glycopolymer p(APMA-b-GAPMA) in this study has molar masses of 19.9 and 25.3 kDa with narrow molecular weight distributions ( $M_w/M_n < 1.30$ ) (see Supporting Information Table S1 and Figure S1). In contrast to APMA homopolymer, cell viability studies revealed that the obtained sugar-containing diblock copolymer, p(APMA<sub>31</sub>-b-GAPMA<sub>45</sub>), shows dramatically reduced toxicity at comparable polymer concentrations (see Supporting Information Figure S2). It is shown that toxicity of the block copolymer can be reduced up to 80%, as compared to that of PAPMA=APMA homopolymer. The cationic glycopolymers were subsequently used in the stabilization of gold nanoparticles. Monodisperse cationic glyconanoparticles were prepared *in situ* by the photoirradiation using Irgacure 2959 as photoinitiator. The photochemical approach for the synthesis of gold nanoparticles was first reported by Scaiano et al., and this method is extensively investigated in our group for both polymer and protein stabilized gold nanoparticles (30–32). The synthesized glyconanoparticles are stabilized by the primary amine pendant groups of the cationic glycopolymer, and therefore, they are expected to be more stable than thiol-stabilized gold nanoparticles due to the oxidative instability of the latter in physiological conditions (33). A recent study reports the physiochemical properties of gold nanoparticles stabilized by tertiary amines; however, detailed *in vitro* studies for this kind of nanoparticles are still to be investigated (33). The gold nanoparticles were synthesized using varying concentrations of polymer and UV radiation in an effort to achieve near-monodisperse cationic glyconanoparticles.

The results obtained by DLS indicated that the optimization of both parameters UV intensity and polymer concentration in solution are crucial to yield monodisperse nanoparticles of about 10 nm in diameter, as shown in Tables 1 and 2.

The gold nanoparticles produced were further analyzed by TEM and UV–vis spectroscopy to confirm the monodispersity of nanoparticles and to further support the DLS data obtained above (Figure 1; Supporting Information Figures S3, S4, S5).

It can be seen that no shift in UV–vis spectrum was observed for the gold nanoparticles produced under different conditions, indicating that nanoparticles produced are of about the same size. TEM images obtained further confirmed the presence of nanoparticles of about 10 nm diameter.

The synthesis of gold nanoparticles was achieved with glycopolymers of molar masses of 19.9 and 25.3 kDa; however, no change in the size of nanoparticles as a function of molecular weight of polymer was observed, possibly due to the small difference in the molecular weight of the two polymers used (Supporting Information Table S3).

The cationic nanoparticles synthesized for *in vitro* gene delivery purposes not only are toxic, but also exhibit the aggregation tendency in biological fluids, due to the interaction of cationic moiety with serum proteins (1). Despite the drawbacks associated with PEGylated systems, the biocompatibility and stabilization of nanoparticles in biological fluid is usually obtained by the incorporation of a PEG layer (1). The cationic glyconanoparticles synthesized were studied for their stability in physiological conditions using DLS and UV–vis spectroscopy. The UV–vis spectrum shows that there is no shift in the spectrum of cationic glyconanoparticles, before and after their dispersion in saline solution and in serum indicating the stability of gold nanoparticles under physiological conditions. These results are in agreement with previously reported serum assay characterization of gold nanoparticles stabilized by cationic glycopolymer p(APMA-b-LAEMA), indicating that regardless of the type of glycopolymer moiety, it is the characteristic of cationic glyconanoparticles to maintain their dispersibility in physiological conditions (29). The quantitative results are then obtained by determining the size of gold nanoparticles before and after their dispersion in saline solution and in human serum by DLS, which show that there is no change in the size of gold nanoparticles before and after their dispersion in saline and in serum (Figure 1 and Supporting Information Table S4).

The study of uptake of cationic glyconanoparticles by Hela cells was performed using confocal microscopy. The TAMARA dye labeled oligonucleotides were complexed with slight excess of p(APMA<sub>31</sub>-b-GAPMA<sub>45</sub>)-f-gold nanoparticles, to ensure the complete complexation of oligonucleotides and the complexes were incubated with Hela cells. The untreated Hela cells and TAMARA labeled oligonucleotides treated Hela cells were used as control (Figure 2).

It is apparent by confocal images that, although most of the nanoparticles seem to localize in the cytoplasm of the cells, few glyconanoparticles can be found entrapped in the endosomes (Figure 2, Supporting Information Figure S6). The presence of some of the nanoparticles in the endosomes of cells can be explained by the fact that the complexation of oligonucleotides with cationic glyconanoparticles is based upon electrostatic interactions. Although most oligos-modified-glyconanoparticles are positively charged due to slight excess of gold nanoparticles in the experiment, a few neutral complexes may form during the process, thus causing their entrapment in endosomes. The enhanced fluorescence images of oligonucleotide-labeled-glyconanoparticle incubated cells, compared to that of controls, confirm that the gene delivery vehicle successfully prevents oligonucleotides from degradation by cytosolic enzymes, even after 3 h of incubation inside the cell. The vesicular escape of

**Table 2. Dynamic Light Scattering Data Showing the Effect of intensity of UV Radiation on the Size of Gold Nanoparticles**

entry	polymer concentration [M]	Au:I:Polymer ratio	intensity (W)	UV time (min)	DLS size (nm)	DLS size distr.
4	$5.1 \times 10^{-6}$	1:3:0.005	224	5	3.3	0.17
5	$5.1 \times 10^{-6}$	1:3:0.005	168	5	4.56	0.10
6	$5.1 \times 10^{-6}$	1:3:0.005	112	5	4.85	0.11
7	$5.1 \times 10^{-6}$	1:3:0.005	56	15	4.73	0.10

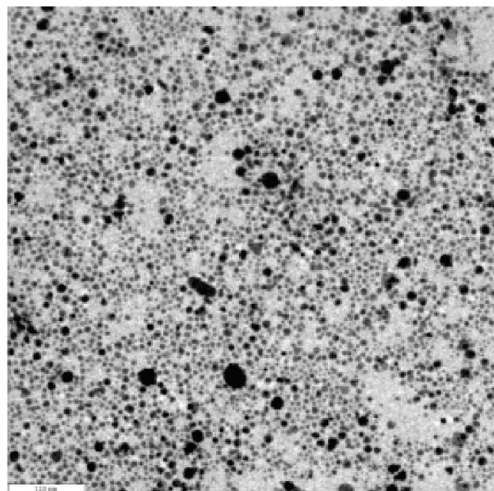
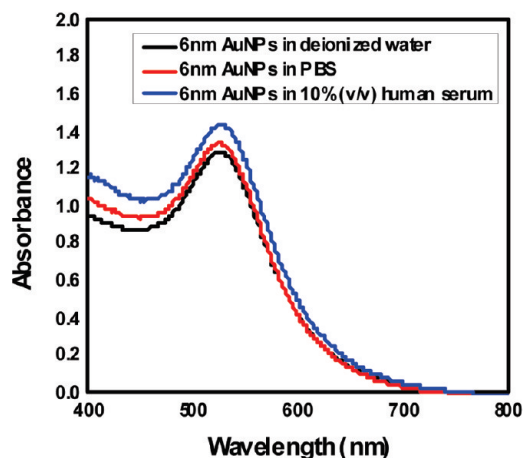


**Figure 1.** Dispersion of  $2.5\ \mu\text{M}$  gold nanoparticles in 10% v/v human serum. TEM micrograph (scale bar — 110 nm) of block copolymer p(APMA<sub>31</sub>-*b*-GAPMA<sub>45</sub>) stabilized gold nanoparticles (entry-1).

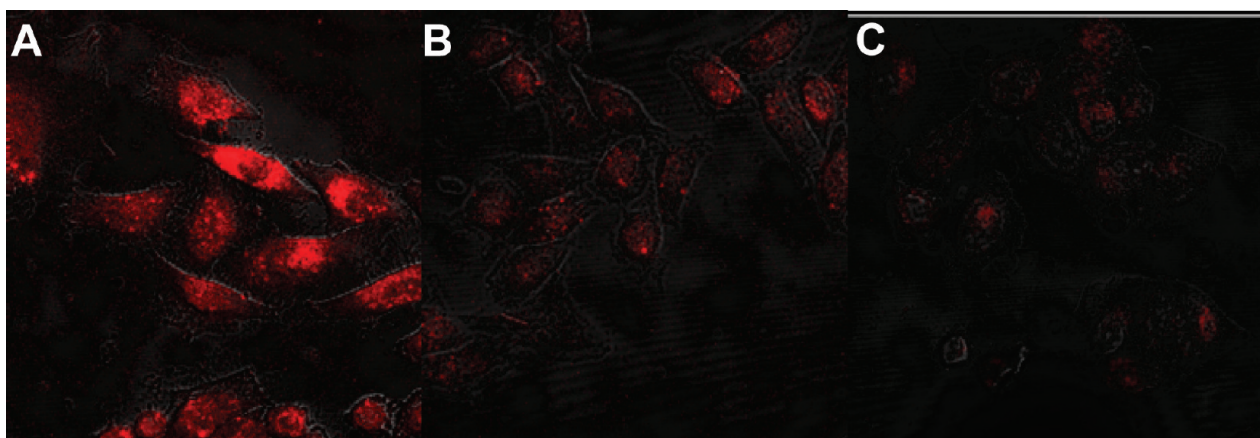


**Figure 2.** Confocal microscopy images of HeLa cells labeled with (A) oligonucleotides complexed p(APMA<sub>31</sub>-*b*-GAPMA<sub>45</sub>)-*f*-gold nanoparticles (entry-2), (B) oligonucleotides, and (C) no treatment.

gene delivery vehicle is apparent by the localization of glyconanoparticles inside the cytoplasm.

The mechanism of uptake of gene delivery carrier is a topic of interest to explore the possible routes adopted by the successful gene delivery vehicles. Funete et al. has compared the interaction of different carbohydrate monomers to the cell surface (27). It has been found that glucose modified glyconanoparticles are not endocytosed (27). The presence of cationic character, in combination with sugar residues, is expected to alter the mechanism of uptake of gold nanoparticles by cells (1). The mechanism of uptake of p(APMA<sub>31</sub>-*b*-GAPMA<sub>45</sub>)-*f*-gold nanoparticles was studied in detail by exploiting energy dependent process of uptake by living cells and it was found that HeLa cells at 4 °C show minimal or no uptake of synthesized nanoparticles, thus indicating that the uptake involves energy dependent processes. To further confirm that the lower uptake of nanoparticles observed at lower temperatures is not due to the physiological malfunctioning of the cells, as the presence of vacuoles in cells treated at lower temperatures is observed, the process was further investigated after the treatment of cells with hypertonic solution at 37 °C (35). The same fluorescently labeled gold nanoparticles were incubated with pretreated cells under the same conditions and the confocal images were obtained. The images show the minimum uptake of gold nanoparticles by HeLa cell after the treatment with hypertonic medium compared to oligonucleotide-modified glyconanoparticle treated cells under normal conditions (Figure 3 and Supporting Information Figure S6).

The z-section images of cells taken from confocal microscope confirm that most of the nanoparticles though can associate themselves around the periphery of cells; they are not endocytosed (see Supporting Information Figure S7). Although a slight change in shape of some of the cells after treatment with hypertonic medium is seen, most of the cells maintain their physiological appearance. It is clear from the figure that cationic glyconanoparticles are capable of cellular interactions in the presence of endocytosis inhibitor, but they are not endocytosed. The cellular attachment of cationic glyconanoparticles can either be considered as a function of glycopolymer interactions to the glycoproteins of plasma membrane, or cationic segments of the nanoparticles can successfully mediate electrostatic interactions with anionic cell membrane. Thus, it can be concluded that the major route of uptake of nanoparticles is found to be receptor mediated endocytosis. It has been reported that uptake of polymer-DNA complexes by receptor mediated endocytosis leads to successful gene delivery (1). The major issue in this regard is the entrapment of gene delivery scaffold in the endocytic vesicles after their successful uptake (1). The localization of most of the nanoparticles in cytosol confirms that glyconanoparticles with net cationic character can successfully disrupt the endocytic vesicles, leading to the release of nanoparticles in the cytoplasm. This is one step forward toward the synthesis of gene delivery vehicles, where some recent works report the localization of vehicles inside the endosomes (4, 36).

The role of cationic glyconanoparticles as a novel gene delivery carrier was explored. The cyanine fluorescence protein-



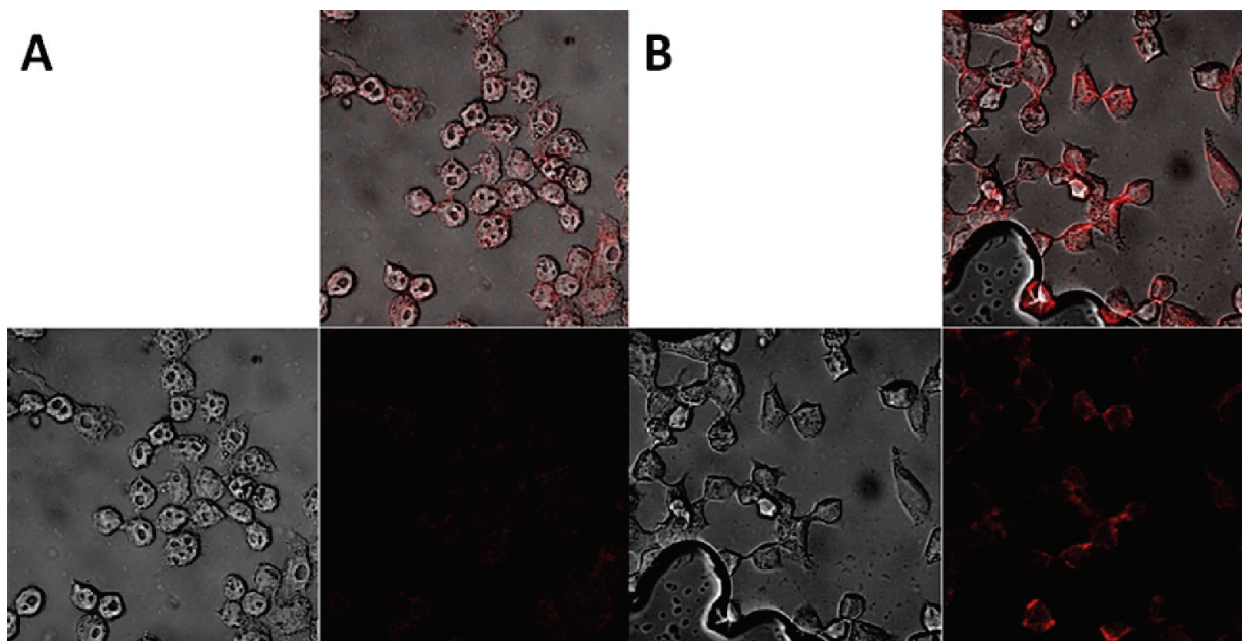


**Figure 3.** Confocal microscopy images of HeLa cells incubated at (A) 4 °C, labeled with oligonucleotide-complexed gold nanoparticles stabilized with p(APMA<sub>31</sub>-b-GAPMA<sub>45</sub>) (entry-2), (B) HeLa cells pretreated with 0.45 M sucrose and incubated with oligonucleotide-complexed gold nanoparticles stabilized with p(APMA<sub>31</sub>-b-GAPMA<sub>45</sub>) at 37 °C.

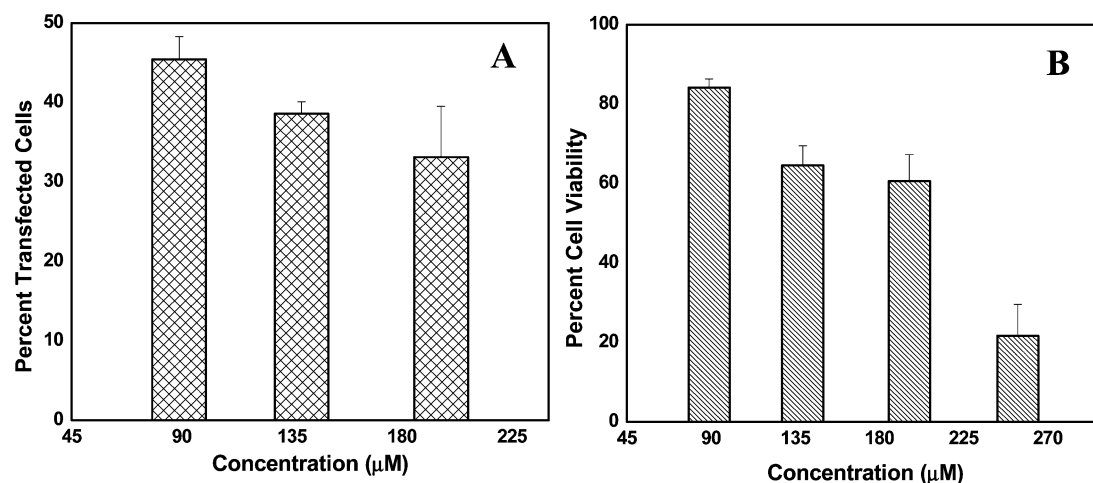


**Figure 4.** The gene transfection efficiencies and cell viability values of HeLa cells upon treatment with cationic glyconanoparticle–plasmid complex. (A) Transfection efficiencies of p(APMA<sub>31</sub>-b-GAPMA<sub>45</sub>)-f-gold nanoparticles in HeLa cells upon their incubation with ECFP plasmid–nanoparticle complex at 37 °C. (B) Normalized viability of HeLa cells transfected with glyconanoparticles–plasmid complex, determined by MTT assay (entry-1).

encoded DNA plasmid (pECFP-N1) was used to study the DNA complexation with the cationic glyconanoparticles by agarose gel electrophoresis. The plasmid is incubated with varying concentrations of p(APMA<sub>31</sub>-b-GAPMA<sub>45</sub>)-f-gold nanoparticles, and it is found that the complete complexation of plasmid is obtained upon incubation with 89 μM gold nanoparticles (see Supporting Information Figures S8 and S9). The migration of complex was completely retarded upon incubation of the plasmid with 89 μM concentration of gold nanoparticles; it can be safely assumed that nanoparticle–plasmid complexes maintain their net cationic character, thus are able to mediate vesicular escape and are resistant to aggregation in physiological conditions.

Finally, the transfection experiments were performed to determine the efficacy of gold nanoparticles *in vitro*. The use of polyplex based nanomaterials for gene delivery purposes is a rapidly advancing field in gene therapy (38–40). Polymer stabilized metallic nanoparticles have also been employed for

gene delivery purposes, and gold, due to its inert nature, is one of the most commonly used metals for this purpose (41). Sandhu et al. have reported the relatively high transfection efficiencies *in vitro* by using amphiphilic gold nanoparticles. However, the process was facilitated with chloroquine, and no cytotoxicity data were provided (7). Others describe significantly low transfection efficiencies of comparatively biocompatible gold nanoparticles based gene delivery scaffolds (8). Wang et al. have reported the transfection efficiency of cyclodextrin modified gold nanoparticles complexed with green fluorescence encoded protein (pEGFP) plasmid in MCF-7 cells. The gene delivery carrier is reported to be 100% cell viable at various N/P ratios; however, the maximum transfection efficiencies obtained are reported to be less than 10% (8). The study of transfection efficiencies of glyconanoparticles of different core sizes has shown that, regardless of the net negative charge on the surface of the complex, gold nanoparticles of 40 nm in core diameter show the highest gene transfection ability compared to the other

sizes of glyconanoparticles. The gold nanoparticles in the study were surface functionalized with cationic glycopolymer p(APMA<sub>31</sub>-*b*-LAEMA<sub>32</sub>) (29). Herein, we report the transfection efficiencies of biocompatible nanoparticles using cationic glycopolymer p(APMA<sub>31</sub>-*b*-GAPMA<sub>45</sub>). The transfection experiments were performed at various concentrations of gold nanoparticles, and the results indicated that transfection efficiencies were not significant compared to control (plasmid alone) when concentration of gold nanoparticles was less than 89  $\mu$ M, possibly due to the net anionic character of the nanoparticles–plasmid complex, as determined by agarose gel electrophoresis. The significant transfection efficiencies (45–50%) with low toxicity values ( $\sim$ 85% cell viability) were observed upon the complexation of plasmid with 89  $\mu$ M gold nanoparticles (Figure 4; see Supporting Information Figure S10).

The improved transfection efficiency of cationic glyconanoparticle–plasmid complexes in the absence of external force is attributed to the net cationic charge of the vehicle, thus leading to successful delivery of gene inside the cells. It should be noted that, despite possessing the same cationic component, the enhanced transfection efficiency of p(APMA-*b*-GAPMA) functionalized gold nanoparticles as compared to p(APMA-*b*-LAEMA) functionalized nanoparticles of the same sizes is attributed to higher glycopolymer component of the polymer (29). These results are in agreement with previous studies, which also show that the glycopolymer component of the carrier largely influences the transfection efficiencies (14).

As expected, further increase in the cationic character does not affect the transfection efficiency of the vehicle significantly, but does lead to significant toxicity to the cells, due to the presence of excess positive charge. These results are in agreement with the previous data where p(APMA-*b*-LAEMA)-*f*-gold nanoparticles of 10 nm core diameter are shown to exhibit the same behavior (29). The transfection efficiencies of novel gene delivery scaffolds were compared to that of commercially available control lipofectamine 2000. The previous experiments showed that lipofectamine can successfully transfect HeLa cells and the transfection efficiency was found to be 55–60% with significant toxicity (20% cell viability). Although the transfection efficacy of glyconanoparticles was comparable to that of lipofectamine, the lower toxicity of glyconanoparticles was an obvious preference over the commercially available standard. Thus, the vehicle presents a desired compromise between two major issues: cell viability and transfection efficacy.

## CONCLUSION

In short, we describe the facile synthesis of cationic glyconanoparticles using photochemistry. The size and polydispersity of gold nanoparticles were controlled by UV radiation and concentration of cationic glycopolymer. The near-monodisperse cationic glyconanoparticles produced were found to be resistant to aggregation in physiological conditions. The mechanism of uptake of this novel gene delivery vehicle was studied, and it was found that cationic nanoparticles produced undergo receptor mediated endocytosis following their vesicular escape, due to the net cationic character of the nanoparticles. Finally, the cationic nanoparticles were complexed with reported plasmid, and their transfection efficacy was determined. The results suggest that biocompatibility of nanoparticles and their easy uptake by cells followed by vesicular escape and nuclear entry, in the absence of external impulse, prove the successful fabrication of a novel type of gene delivery vehicle.

## ACKNOWLEDGMENT

The author would like to thank Natural Sciences and Engineering Research Council of Canada for financial support of this research work.

**Supporting Information Available:** GPC and <sup>1</sup>H NMR data of block copolymer synthesis, toxicity results of the polymers, DLS data and agarose gel electrophoresis for the complexation of DNA to gold nanoparticles, confocal images of gold nanoparticles uptake by HeLa cells, and transfection images. This material is available free of charge via the Internet at <http://pubs.acs.org>.

## LITERATURE CITED

- (1) Mintzer, A. M., and Simanek, E. E. (2009) Nonviral vectors for gene delivery. *Chem. Rev.* 109, 259–302.
- (2) Srinivasachari, S., Liu, Y., Zhang, G., Prevette, L., and Reineke, M. T. (2006) Trehalose click polymers inhibit nanoparticle aggregation and promote pDNA delivery in serum. *J. Am. Chem. Soc.* 128, 8176–8184.
- (3) Sharma, R., Lee, S.-J., Bettencourt, C. R., Xiao, C., Konieczny, F. S., and Won, Y.-Y. (2008) Effects of the incorporation of a hydrophobic middle block into a PEG-polycation diblock copolymer on the physicochemical and cell interaction properties of the polymer–DNA complexes. *Biomacromolecules* 9, 3294–3307.
- (4) Pun, S. H., and Davis, E. M. (2002) Development of a nonviral gene delivery vehicle for systemic application. *Bioconjugate Chem.* 13, 630–639.
- (5) Kostarelos, K., and Miller, D. A. (2005) Synthetic, self-assembly ABCD nanoparticles; a structural paradigm for viable synthetic non-viral vectors. *R. Soc. Chem.: Chem Soc. Rev.* 34, 970–994.
- (6) Lomas, H., Massignani, M., Abdullah, A. K., Canton, I., Presti, L. C., MacNiel, S., Du, J., Blazas, A., Madsen, J., Armes, P. S., Lewis, L. A., and Battaglia, G. (2008) Non-cytotoxic polymer vesicles for rapid and efficient intracellular delivery. *Faraday Discuss.* 139, 143–159.
- (7) Snadhu, K. K., McIntosh, M. C., Simard, M. J., Smith, W. S., and Rotello, M. V. (2002) Gold nanoparticle-mediated transfection of mammalian cells. *Bioconjugate Chem.* 13, 3–6.
- (8) Wang, H., Chen, Y., Li, X.-Y., and Liu, Y. (2007) Synthesis of Oligo(ethylenediamino)- $\beta$ -cyclodextrin modified gold nanoparticle as a DNA concentrator. *Mol. Pharmaceutics* 4, 189–198.
- (9) Strand, P. S., Issa, M. M., Christensen, E. B., Varum, M. K., and Artursson, P. (2008) Tailoring of chitosans for gene delivery: novel self-branched glycosylated chitosan oligomers with improved functional properties. *Biomacromolecules* 9, 3268–3276.
- (10) Gao, K., and Huang, L. (2008) Nonviral methods for siRNA delivery. *Mol. Pharmaceutics* 6, 651–658.
- (11) Thompson, H. D. (2008) Adenovirus in a synthetic membrane wrapper: an example of hybrid virus. *ACS Nano* 2, 821–826.
- (12) Bergen, J. M., Recum, H. A., Goodman, T. T., Massey, P. A., and Pun, S. H. (2006) Gold nanoparticles as a versatile platform for optimizing physicochemical parameters for targeted drug delivery. *Macromol. Biosci.* 6, 506–516.
- (13) Saul, M. J., Wang, H. C.-H., Ng, P. C., and Pun, S. H. (2008) Multilayer nanocomplexes of polymer and DNA exhibit enhanced gene delivery. *Adv. Mater.* 20, 19–25.
- (14) Liu, Y., Wenning, L., Lynch, M., and Reineke, M. T. (2004) New poly(D-glucaramidoamine)s induce DNA nanoparticle formation and efficient gene delivery into mammalian cells. *J. Am. Chem. Soc.* 126, 7422–7423.
- (15) Ghosh, S. P., Kim, C. K., Han, G., Forbes, S. N., and Rotello, M. V. (2008) Efficient gene delivery vectors by tuning the surface charge density of amino acid-functionalized gold nanoparticles. *ACS Nano* 2, 2213–2218.
- (16) Li, P., Li, D., Zhang, L., Li, G., and Wang, E. (2008) Cationic lipid bilayer coated gold nanoparticles-mediated transfection of mammalian cells. *Biomaterials* 29, 3617–3624.
- (17) Zhou, X., Zhang, X., Yu, X., Zha, X., Fu, Q., Liu, B., Wang, X., Chen, Y., Chen, Y., Shan, Y., Jin, Y., Wu, Y., Liu, J., Kong,

- W., and Shen, J. (2008) The effect of conjugation to gold nanoparticles on the ability of low molecular weight chitosan to transfer DNA vaccine. *Biomaterials* 29, 111–117.
- (18) Zheng, M., Li, Z., and Huang, X. (2004) Ethylene glycol monolayer protected nanoparticles: synthesis, characterization, and interactions with biological molecules. *Langmuir* 20, 4226–4235.
- (19) Li, Z.-P., Wang, Y.-C., Liu, H.-C., and Li, Y.-K. (2005) Development of chemiluminescence detection of gold nanoparticles in biological conjugates for immunoassay. *Anal. Chim. Acta* 551, 85–91.
- (20) Shimmin, G. R., Schoch, B. A., and Braun, V. P. (2004) Polymer size and concentration effects on the size of gold nanoparticles capped by polymeric thiols. *Langmuir* 20, 5613–5620.
- (21) Guo, R., Zhang, L., Zhu, Z., and Jiang, X. (2008) Direct facile approach to the fabrication of chitosan-gold hybrid nanospheres. *Langmuir* 24, 3459–3464.
- (22) Das, j., Huh, C.-H., Kwon, K., Park, S., Jon, S., Kim, K., and Yang, H. (2009) Comparison of the nonspecific binding of DNA-conjugated gold nanoparticles between polymeric and monomeric self-assembled monolayers. *Langmuir* 25, 235–241.
- (23) Ganguli, M., Babu, V. J., and Maiti, S. (2004) Complex formation between cationically modified gold nanoparticles and DNA: an atomic force microscopic study. *Langmuir* 20, 5165–5170.
- (24) Leroueil, R. P., Berry, A. S., Duthie, K., Han, G., Rotello, M. V., McNerny, Q. D., Baker, R. J., Orr, G. B., and Banaszak Holl, M. M. (2008) Wide varieties of cationic nanoparticles induce defects in supported lipid bilayers. *Nano Lett.* 8, 420–424.
- (25) (a) De la Fuente, M. J., Barrientos, G. A., Rojas, C. T., Rojo, J., Canada, J., Fernandez, A., and Penades, S. (2001) Gold glyconanoparticles as water-soluble polyvalent models to study carbohydrate interactions. *Angew. Chem.* 113, 2318–2321.
- (26) Barrientos, G. A., De la Fuente, M. J., Rojas, C. T., Fernandez, A., and Penades, S. (2003) Gold glyconanoparticles: synthetic polyvalent ligands mimicking glycocalyx-like surfaces as tools for glycobiological studies. *J. Chem. Eur.* 9, 1909–1921.
- (27) Fuente, M. J., Alcantara, D., and Penades, S. (2007) Cell response to magnetic glyconanoparticles: does the carbohydrate matter? *IEE Trans. Nanobiosci.* 6, 275–281.
- (28) Funete de la, M. J., and Berry, C. C. (2005) Tat peptide as an efficient molecule to translocate gold nanoparticles into the cell nucleus. *Bioconjugate Chem.* 16, 1176–1180.
- (29) Ahmed, M., Deng, Z., and Narain, R. (2009) Study of transfection efficiencies of gold nanoparticles of different core sizes. *ACS Appl. Mater. Interfaces* ASAP.
- (30) Mcgilvray, L. K., Decan, R. M., Wang, D., and Scaiano, C. J. (2006) Facile photochemical synthesis of unprotected aqueous gold nanoparticles. *J. Am. Chem. Soc.* 128, 15980–15981.
- (31) Narain, R., Housni, A., Gody, G., Boullanger, P., Charreyre, M., and Delair, T. (2007) Preparation of biotinylated glyconanoparticles via a photochemical process and study of their bioconjugation to streptavidin. *Langmuir* 23, 12835–12841.
- (32) Housni, A., Ahmed, M., Liu, S., and Narain, R. (2008) Monodisperse Protein Stabilized Gold Nanoparticles via a Simple Photochemical Process. *J. Phys. Chem. C* 112, 12282–12290.
- (33) Miyamoto, D., Oishi, M., Kojima, K., Yoshimoto, K., and Nagasaki, Y. (2008) Completely dispersible PEGylated gold nanoparticles under physiological conditions: modification of gold nanoparticles with precisely controlled PEG-b-polyamine. *Langmuir* 24, 5010–5017.
- (34) Wang, Z., Tan, B., Hussain, I., Schaeffer, N., Wyatt, F. M., Brust, M., and Cooper, I. A. (2007) Design of polymeric stabilizers for size-controlled synthesis of monodisperse gold nanoparticles in water. *Langmuir* 23, 885–895.
- (35) Heuser, E. J., and Anderson, W. G. R. (1989) Hypertonic media inhibit receptor-mediated endocytosis by blocking clathrin-coated pit formation. *J. Cell Biol.* 108, 389–400.
- (36) Yin, M., Ding, K., Gropeanu, A. R., Shen, J., Berger, R., Weil, T., and Mullen, K. (2008) Dendritic star polymers for efficient DNA binding and stimulus-dependent DNA release. *Biomacromolecules* 9, 3231–3238.
- (37) Deng, Z., Bouchekif, H., Babooram, K., Housni, A., Choytun, N., and Narain, R. (2008) Facile synthesis of controlled-structure primary amine-based methacrylamide polymers via the reversible addition-fragmentation chain transfer process. *J. Polym. Sci., Part A: Polym. Chem.* 46, 4984–4996.
- (38) Zhang, X., Sharma, K. K., Boeglin, M., Ogier, J., Mainard, D., Voegel, J.-C., Mely, V., and Benkirane-Jessel, N. (2008) Transfection ability and intracellular DNA pathway of nanostructured gene-delivery systems. *Nano Lett.* 8, 2432–2436.
- (39) Meyer, M., Dohmen, C., Philipp, A., Kiener, D., Maiwald, G., Scheu, C., Ogris, M., and Wagner, M. (2009) Synthesis and biological evaluation of bioresponsive and endosomolytic siRNA-polymer conjugate. *Mol. Pharmaceutics* 6, 752–762.
- (40) York, W. A., Zhang, Y., Holley, C. A., Guo, Y., Huang, F., and McCormick, L. C. (2009) Facile synthesis of multivalent folate-block copolymer conjugates via aqueous RAFT polymerization: targeted delivery of siRNA and subsequent gene suppression. *Biomacromolecules* 10, 936–943.
- (41) Koda, S., Inoue, Y., and Iwata, H. (2008) Gene transfection into adherent cells using electroporation on a dendrimer modified gold electrode. *Langmuir* 24, 13525–13531.

BC900350C